

Nonlinear Schrödinger Equation with Spatio-Temporal Perturbations

Franz G. Mertens

Physikalisches Institut, Universität Bayreuth, 95440 Bayreuth, Germany

Niurka R. Quintero

Departamento de Física Aplicada 1, E.U.P. Universidad de Sevilla, Virgen de África 7, 41011 Sevilla, Spain

A. R. Bishop

*Theoretical Division and Center for Nonlinear Studies,
Los Alamos National Laboratory, Los Alamos, NM 87545, USA*

We investigate the dynamics of solitons of the cubic Nonlinear Schrödinger Equation (NLSE) with the following perturbations: non-parametric spatio-temporal driving of the form $f(x,t) = a \exp[iK(t)x]$, damping, and a linear term which serves to stabilize the driven soliton. Using the time evolution of norm, momentum and energy, or, alternatively, a Lagrangian approach, we develop a Collective-Coordinate-Theory which yields a set of ODEs for our four collective coordinates. These ODEs are solved analytically and numerically for the case of a constant, spatially periodic force $f(x)$. The soliton position exhibits oscillations around a mean trajectory with constant velocity. This means that the soliton performs, on the average, a unidirectional motion although the spatial average of the force vanishes. The amplitude of the oscillations is much smaller than the period of $f(x)$. In order to predict for which regions the above solutions are stable, we calculate the relationship $P(V)$ where P and V are the soliton momentum and velocity. If the curve $P(V)$ has a branch with negative slope, the soliton is expected to become unstable, which is confirmed by our simulations for the perturbed NLSE. Moreover, this curve also yields a good estimate for the soliton lifetime: the soliton lives longer, the shorter the branch with negative slope is.

I. INTRODUCTION

The Nonlinear Schrödinger Equation (NLSE) is one of the paradigms of soliton physics, because it represents a completely integrable system and has very many applications in practically all fields of physics, which are listed and discussed in several review articles [1, 2, 3]. For applications it is important to study the perturbed NLSE

$$iu_t + u_{xx} + 2|u|^2u = R[u(x,t); x,t]. \quad (1)$$

Many different kinds of perturbations R were considered and in particular the dynamics of a single soliton under these perturbations was investigated [1, 2].

In this paper we consider the following combination of perturbations

$$R = f(x,t) - i\beta u(x,t) - \delta u(x,t) \quad (2)$$

with the real parameters β and δ and the *non-parametric spatio-temporal* driving force

$$f(x,t) = ae^{iK(t)\cdot x}, \quad (3)$$

which yields several interesting effects, as we will see. The literature so far has mostly dealt with parametric driving [1, 2, 4, 5, 6, 7]. Non-parametric (external) driving was studied without space dependence, e. g., $f = \epsilon \exp(i\omega t)$ [8, 9, 10], and with a periodic space dependence, e.g., $f = \epsilon \exp[i(kx - \omega t)]$ [11, 12]. Moreover, $f = \epsilon \exp[ig(x,t) - i\omega t]$, where g is a function of $x - vt$, was considered, but no localized solutions were discussed [12].

Our driving term in (3) was already used in the discrete form $f = a \exp[in\phi(t)]$. Here the integer n denotes a lattice site in a nonlinear optical waveguide array which is modeled by a Discrete Nonlinear Schrödinger Equation [13]. $\phi(t)$ is the incident angle of a laser beam. In order to get a ratchet effect, a biharmonic $\phi(t)$ was used which breaks a temporal symmetry.

In our paper we work with an arbitrary function $K(t)$ in the driving term (3) and develop a Collective Coordinate (CC) Theory for the soliton dynamics which results in a set of nonlinear coupled ODEs for the CCs (Sections II and III). In order to obtain analytical and numerical solutions we then consider the case of temporally constant, spatially periodic driving $f(x) = a \exp(iKx)$ with constant K (Section IV). Although the spatial average of $f(x)$ vanishes there is transport: the soliton performs a unidirectional motion on the average, in contrast to the case of parametric driving $R = \epsilon \cdot u(x, t) \cdot V(x)$ with a periodic potential $V(x)$ in which the soliton performs an oscillatory motion around a minimum of $V(x)$ [6]. Solutions of the CC-Eqs. for the case of a harmonic or biharmonic time dependence of $K(t)$ will be presented in a second paper.

The second term, $-i\beta u(x, t)$ with $\beta > 0$, in the perturbation (2) is a damping term which allows us to obtain a balance between the energy input from the driving and the dissipation. The third term, $-\delta u(x, t)$, in Eq. (2) will turn out to be decisive for the stability of the driven soliton. For $\delta \geq 0$ the soliton radiates phonons (i.e., linear excitations) and eventually vanishes, or even breaks up into several solitons. For $\delta < 0$ the situation is more complicated and will be discussed below.

Section V presents a stable and an unstable stationary solution for the case without damping. For the region around the stable solution the CC-theory yields solutions in which all CCs exhibit oscillations with the same intrinsic frequency Ω , which can be calculated approximately. However, tests by simulations, i.e. numerical solutions of the perturbed NLSE, reveal that the oscillatory solutions are stable only for certain regions of the initial conditions. These regions become broader when δ is chosen more negative (Section VI).

The stability regions can be calculated by the CC-theory using the stability criterion of Pego and Weinstein [14], although this criterion was not established for NLS-equations but for several classes of other soliton bearing equations. (The NLS stability criterion of Vakhikov and Kolokolov [15, 16] cannot be applied to our oscillatory solutions).

The Pego-Weinstein criterion states that the soliton is unstable if $dP/dV < 0$, where P and V are the soliton momentum and velocity, respectively. Interestingly, the curve $P(V)$ not only predicts whether the soliton is unstable, but it also allows us to estimate the soliton lifetime: This time is longer, the shorter the branch with negative slope is (Section VI).

Finally we show in Section VII that the kinetic and canonical soliton momenta are identical, and we analytically calculate the soliton and phonon dispersion curves.

II. TIME EVOLUTION OF NORM, MOMENTUM, AND ENERGY

Multiplication of the perturbed NLSE (1) by u^* and subtraction of the complex conjugate NLSE multiplied by u yields

$$\frac{\partial \varrho}{\partial t} + \frac{\partial j}{\partial x} = i(R^*u - Ru^*) \quad (4)$$

with the density and current density

$$\varrho = |u|^2, \quad j = i(u_x^*u - u^*u_x). \quad (5)$$

By integration of Eq.(4) over x , assuming decaying boundary conditions, we obtain the time evolution of the norm,

$$N = \int_{-\infty}^{+\infty} dx |u|^2, \quad (6)$$

which is

$$\dot{N} = i \int_{-\infty}^{+\infty} dx (R^* u - R u^*) \quad (7)$$

$$= -2\beta N + i \int_{-\infty}^{+\infty} dx (f^* u - f u^*), \quad (8)$$

where the terms with δ have dropped out.

Multiplication of Eq. (1) by u_x^* , addition of the complex conjugate equation multiplied by u_x , and integration over x yields the time evolution of the momentum

$$\dot{P} = \int_{-\infty}^{+\infty} dx (R^* u_x + R u_x^*) \quad (9)$$

where P is defined as

$$P = \frac{i}{2} \int_{-\infty}^{+\infty} dx (u u_x^* - u^* u_x). \quad (10)$$

Multiplication of Eq. (1) by u_t^* , addition of the complex conjugate equation multiplied by u_t , and integration yield the time evolution of the energy

$$\dot{E} = - \int_{-\infty}^{+\infty} dx (R^* u_t + R u_t^*), \quad (11)$$

where

$$E = \int_{-\infty}^{+\infty} dx [|u_x|^2 - |u|^4]. \quad (12)$$

Interestingly, for $\beta = 0$ and time independent force, i. e. $R = f(x) - \delta u$, the r.h.s. of Eq. (11) can be written as a time derivative

$$\dot{E} = - \frac{\partial}{\partial t} \int_{-\infty}^{+\infty} dx [f^* u + f u^* - \delta |u|^2]. \quad (13)$$

Thus the *perturbed* NLSE (1) without damping possesses a conserved quantity for *arbitrary* $f(x)$

$$E^{tot} = \int_{-\infty}^{+\infty} dx [|u_x|^2 - |u|^4 - \delta |u|^2 + f^* u + f u^*]. \quad (14)$$

$f(x)$ can be interpreted as a constant (external) force, in contrast to the case of parametric driving $R = \epsilon u \cdot V(x)$, where $V(x)$ can be understood as a potential (in which the solitons move). In this case the conserved quantity is [6]

$$E_{para}^{tot} = \int_{-\infty}^{+\infty} dx [|u_x|^2 - |u|^4 + \epsilon V(x) |u|^2]. \quad (15)$$

In Sections IV and V we will show that a soliton under a constant *periodic* force $f(x) = a \exp(iKx)$ performs, on the average, a *unidirectional* motion, although the average of f vanishes.

When we include the damping ($\beta > 0$), the time evolution of the total energy is

$$\dot{E}^{tot} = -\beta \int_{-\infty}^{+\infty} dx [2|u_x|^2 - 4|u|^4 - 2\delta |u|^2 + f^* u + f u^*]. \quad (16)$$

III. COLLECTIVE COORDINATE THEORY

The 1-soliton solution of the unperturbed NLSE reads [1]

$$u(x, t) = 2i\eta \operatorname{sech}[2\eta(x - \zeta)]e^{-i(2\xi x + \phi)} \quad (17)$$

with the real parameters $\eta > 0$ and ξ , the soliton position

$$\zeta(t) = \zeta_0 - 4\xi t, \quad (18)$$

and the phase of the internal oscillation

$$\phi(t) = \phi_0 + 4(\xi^2 - \eta^2)t. \quad (19)$$

The soliton has amplitude 2η , width $1/(2\eta)$, velocity $V = -4\xi$ and phase velocity of the carrier wave $V_{ph} = -2\xi + 2\eta^2/\xi$.

Including the term with δ on the r.h.s. of Eq. (1), only the phase is changed:

$$\phi(t) = \phi_0 + [4(\xi^2 - \eta^2) - \delta]t. \quad (20)$$

For this reason the term with δ need not be treated as a perturbation and will be counted among the unperturbed parts of the NLSE in the following

$$iu_t + u_{xx} + 2|u|^2 + \delta u = f(x, t) - i\beta u. \quad (21)$$

Therefore we now define the energy as

$$E = \int_{-\infty}^{+\infty} dx [|u_x|^2 - |u|^4 + \delta|u|^2], \quad (22)$$

which is conserved for the unperturbed NLSE. Using Eq. (17) we obtain the soliton energy

$$E^{sol} = 16\eta\xi^2 - \frac{16}{3}\eta^3 - 4\delta\eta. \quad (23)$$

For the discussion of the stability of the perturbed soliton the above definition will turn out to be more suitable than a definition without the δ -term (Section VII).

The definitions (6) and (10) need not be changed, because all terms with δ drop out on the r.h.s. of Eq. (8) and (9). The norm and the momentum of the soliton are, respectively,

$$N = 4\eta; P = -8\eta\xi. \quad (24)$$

Writing $P = MV$, the soliton mass is related to the norm by $M = N/2$.

From the Inverse Scattering Theory (IST) it is well known [1] that a perturbation theory results in a time dependence of η and ξ and in a change of the simple time dependence of ζ and ϕ in Eqs. (18) and (19). Therefore we take Eq. (17) as an ansatz with the four Collective Coordinates (CCs) $\eta(t)$, $\xi(t)$, $\zeta(t)$ and $\phi(t)$ and insert it into Eqs. (8), (9) and (11), using $f(x, t) = a \exp[iK(t) \cdot x]$ from Eq. (3).

Eq. (8) yields

$$\dot{\eta} = -2\beta\eta - a\frac{\pi}{2}\operatorname{sech}A \cdot \cos B \quad (25)$$

with

$$A(t) = \frac{\pi}{4}[K(t) + 2\xi(t)]/\eta(t) \quad (26)$$

$$B(t) = \phi(t) + [K(t) + 2\xi(t)]\zeta(t). \quad (27)$$

Two of the three terms which result on the r.h.s. of (9) cancel with the term $-8\eta\xi$ on the l.h.s.. The remaining terms are

$$\dot{\xi} = aA \operatorname{sech}A \cdot \cos B. \quad (28)$$

Finally, Eq. (11) gives $8\eta\dot{\xi}\{\dots\} - 4\dot{\eta}\{\dots\} = 0$ which can be solved by setting the curly brackets to zero:

$$\dot{\zeta} = -4\xi + \frac{a\pi^2}{8\eta^2} \operatorname{sech}A \cdot \tanh A \cdot \sin B, \quad (29)$$

$$\dot{\phi} + 2\zeta\dot{\xi} = 4(\xi^2 - \eta^2) - \delta + \frac{a\pi A}{2\eta} \operatorname{sech}A \cdot \tanh A \cdot \sin B. \quad (30)$$

Possibly Eqs. (29) and (30) are not the only solution, therefore we alternatively use the Lagrangian method which will also be useful for section VII. Our perturbed NLSE is equivalent to an Euler-Lagrange-Equation, generalized by a dissipative term,

$$\frac{d}{dt} \frac{\partial \mathcal{L}}{\partial u_t^*} + \frac{d}{dx} \frac{\partial \mathcal{L}}{\partial u_x^*} - \frac{\partial \mathcal{L}}{\partial u^*} = \frac{\partial \mathcal{F}}{\partial u_t^*} \quad (31)$$

with the Lagrangian density

$$\mathcal{L} = \frac{i}{2}(u_t u^* - u_t^* u) - |u_x|^2 + |u|^4 + \delta |u|^2 - f u^* - f^* u \quad (32)$$

and the dissipation function

$$\mathcal{F} = i\beta(u u_t^* - u^* u_t). \quad (33)$$

Inserting our CC-ansatz and integrating over the system we get the CC-Lagrangian

$$L = 4\eta\dot{\phi} + 8\eta\zeta\dot{\xi} - 16\eta\xi^2 + \frac{16}{3}\eta^3 + 4\delta\eta - 2\pi a \operatorname{sech}A \cdot \sin B \quad (34)$$

and the CC-dissipation function

$$F = -\beta(8\eta\dot{\phi} + 16\eta\zeta\dot{\xi}). \quad (35)$$

The CC-equations are then obtained by the four generalized Lagrange equations

$$\frac{d}{dt} \frac{\partial L}{\partial \dot{\psi}} - \frac{\partial L}{\partial \psi} = \frac{\partial F}{\partial \dot{\psi}}, \quad (36)$$

where ψ stands for the four CCs η, ξ, ζ and ϕ . The resulting four ODEs are identical with the Eqs. (25), (28), (29) and (30).

Finally we evaluate Eq. (14), yielding

$$E^{tot} = 16\eta\xi^2 - \frac{16}{3}\eta^3 - 4\delta\eta + 2\pi a \operatorname{sech}A \cdot \sin B. \quad (37)$$

Here the first three terms are the soliton energy (23), while the last term stems from the perturbations. We note that E^{tot} is conserved only in the case of no damping ($\beta = 0$) and time independent force $f(x) = a \exp(iKx)$ with constant K , see below Eq. (13).

IV. CONSTANT, SPATIALLY PERIODIC FORCE

We consider this case because it exhibits some surprising, counter-intuitive features: E. g., the soliton position performs oscillations on a length scale that is very different from the spatial period L of the force.

We take a constant K in Eq. (3), i. e. $f(x) = a \exp(iKx)$, and consider only small values of $|K|$ such that the period $L = 2\pi/|K|$ is much larger than the soliton width. We first consider the case with damping ($\beta > 0$) for which we can expect a steady-state solution for times much larger than a transient time τ on the order of $1/\beta$.

The transformation $u(x, t) = \Psi(X, t) \exp(iKx)$ into a moving frame $X = x - V_f t$ with $V_f = 2K$ leads to the autonomous equation

$$i\Psi_t + \Psi_{XX} + 2|\Psi|^2\Psi = a + (K^2 - \delta)\Psi - i\beta\Psi, \quad (38)$$

with the non-parametric and parametric driving terms a and $(K^2 - \delta)\Psi$, respectively. Apart from the factor $K^2 - \delta := c^2$, which can be eliminated by scaling time by c^2 , space by $c > 0$, and Ψ by $1/c$, Eq. (38) is the same as an autonomous equation, which was obtained from the NLSE (1) with $R = \epsilon \exp(i\omega t) - i\beta u$ by the substitution $u = \Psi(x, t) \exp(i\omega t)$, setting $\omega = 1$ [9, 10]. However, these investigations differ from ours in several respects: In Ref. [9] static soliton solutions of Eq. (38) were obtained numerically, then an existence and stability chart was constructed on the (a, β) plane. In Ref. [10] a singular perturbation expansion was performed at the soliton's existence threshold. In contrast, we study moving solitons by solving our CC-equations, and test the results by simulations, i.e. by numerically solving the NLSE (1). Besides the steady-state solution for $\beta > 0$ (this section), for the case $\beta = 0$ we study stationary solutions and oscillatory solutions, which have a more complicated time dependence (Section V).

The CC-equations from the previous section yield a steady-state solution, in which the driving is compensated by the damping, using the ansatz $\zeta = \zeta_0 + V_f t$ and constant η , ξ , and ϕ :

$$u_f(x, t) = 2i\eta_f \operatorname{sech}\{2\eta_f[x - \zeta(t)]\} e^{i(Kx - \phi_f)}, \quad (39)$$

with

$$\eta_f = \sqrt{K^2 - \delta}/2, \quad (40)$$

$$\phi_f = (2n + 1)\frac{\pi}{2} + \arcsin \frac{4\beta\eta_f}{\pi a}, \quad (41)$$

where n is an integer. This soliton has an internal structure due to the factor $\exp(iKx)$, but no internal oscillations since ϕ_f is constant. In the moving frame the soliton is quiescent and has no internal structure.

In order to confirm this result we have numerically solved the CC-equations for many sets of initial conditions (IC) η_0, ζ_0, ξ_0 and ϕ_0 . The solitons always evolve to the steady-state solution (39), except when the values of η_0, ξ_0 and ϕ_0 are too far from those of the steady-state solution and when the damping β is too large. An example for this is the parameter set $a = 0.05$, $K = 0.01$, $\delta = -3$, $\beta \geq \beta_c \approx 0.003$ with the IC $\eta_0 = 1$, $\xi_0 = \zeta_0 = \phi_0 = 0$. Here the soliton vanishes, i.e. its amplitude and energy go to zero while its width goes to infinity. In order to get a convergence to the steady-state solution one can either reduce β below the critical value β_c (which depends on the other parameters and the IC), or go closer to $\eta_f = 0.8660$ by reducing η_0 by 0.1, for instance, or go closer to ϕ_f by choosing $\phi = \pi/2$.

In this context it is interesting to consider the total energy (37) and its time derivative in which the CC-equations can be inserted. Using MATHEMATICA [17] we obtain

$$\dot{E}^{tot}(t) = -\beta\{8\eta[4(\xi^2 - \eta^2) - \delta] + 4\pi A \operatorname{sech} A \cdot \tanh A \cdot \sin B\}. \quad (42)$$

This is indeed zero for the steady-state solution because $\xi_f = -K/2$ and thus $A \equiv 0$. On the path to that solution, Eq. (42) alternately exhibits both signs. I. e., the total energy performs oscillations which become smaller and smaller while approaching the final value E_f^{tot} .

According to Eq. (40), $\delta < K^2$. As we choose $|K| \ll 1$ (see above), δ is either positive but very small, or δ is negative. This results from the CC-theory; in section VII we will show that the driven soliton can be stable only for $\delta < 0$, by taking into account the phonon modes.

The quality of the CC-theory must be tested by simulations. The soliton shape agrees very well (Fig. 1), but in the simulations the soliton resides on a small constant background because the perturbation $f(x) = a \exp(iKx)$ does not vanish far away from the soliton. This background is

$$u_{bg} = -\frac{a}{\omega_K} e^{iKx}, \quad (43)$$

with $\omega_K = K^2 - \delta - i\beta$; see also the last term in Eq. (78). Plotting the real and imaginary parts of u , the spatial period $L = 2\pi/|K|$ is observed. The norm density $|u|^2$ forms a shelf on which the soliton moves; the shelf height is quantitatively confirmed. The dynamics of the soliton is practically not affected by the background: the time evolution of the soliton position is identical in the CC-theory and the simulations (Fig. 2, right panel); only the soliton amplitude differs a little (left panel).

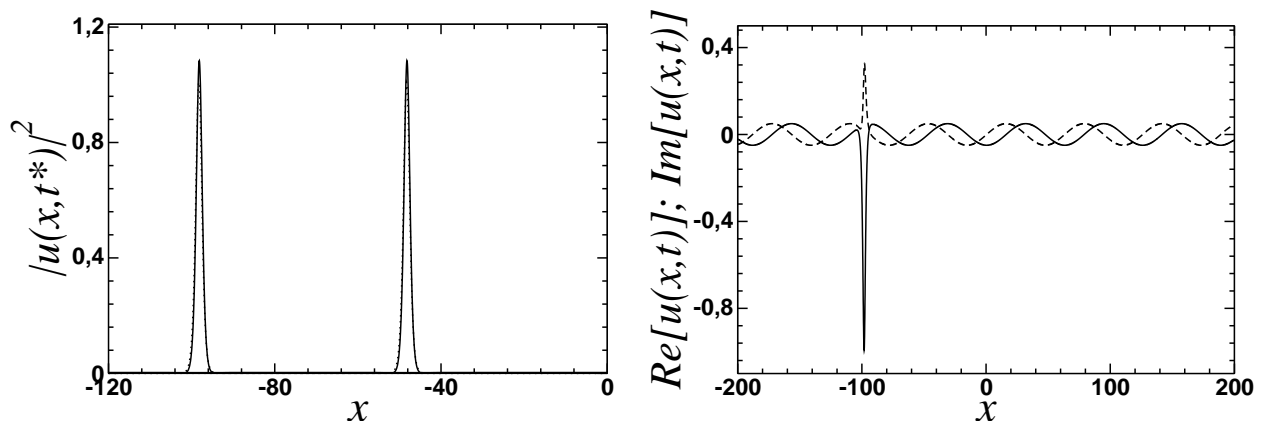


FIG. 1: Left panel: Soliton moving to the left for $t^* = 250, 500$. Simulations of NLSE (solid lines) and numerical solutions of CC-equations (dotted lines). Right panel: Real (solid line) and imaginary (dashed line) parts of $u(x, t)$ for $t = 500$. Parameters: $K = -0.1$, $a = 0.05$, $\delta = -1$, $\beta = 0.05$, with IC $\xi_0 = 0$, $\zeta_0 = 0$, $\phi_0 = 1.69$ and $\eta_0 = 0.5$.

All CCs exhibit decreasing oscillations with an intrinsic frequency Ω which will be discussed in the next section. However, oscillations are not visible in the soliton position $\zeta(t)$ in Fig. 2 because the linear term dominates the time evolution. By reducing the damping β and by choosing a smaller time scale one can see the oscillations also in $\zeta(t)$, see Fig. 3.

In any case, the soliton performs, on the average, a unidirectional motion although the spatial average of the periodic force $f(x) = a \exp(iKx)$ is zero. This is a ratchet-like system in which the translational symmetry is broken by the inhomogeneity $f(x)$ in the NLS-equation.

Interestingly, the period $L = 2\pi/|K|$ of the inhomogeneity $f(x)$ does not show up in the soliton dynamics: For early times ($t \leq \tau = O(1/\beta)$) the soliton performs the above mentioned oscillations around the mean trajectory $\zeta = Vt$. However, the amplitude of these oscillations is much smaller than L (e.g., $L = 62.8$ for $K = 0.1$). When the strength a of the inhomogeneity is strongly increased ($a = 1$, for instance), $\zeta(t)$ exhibits a staircase structure. The height of the steps is larger than the amplitude of the above oscillations, but still much smaller than L . However, such values of a

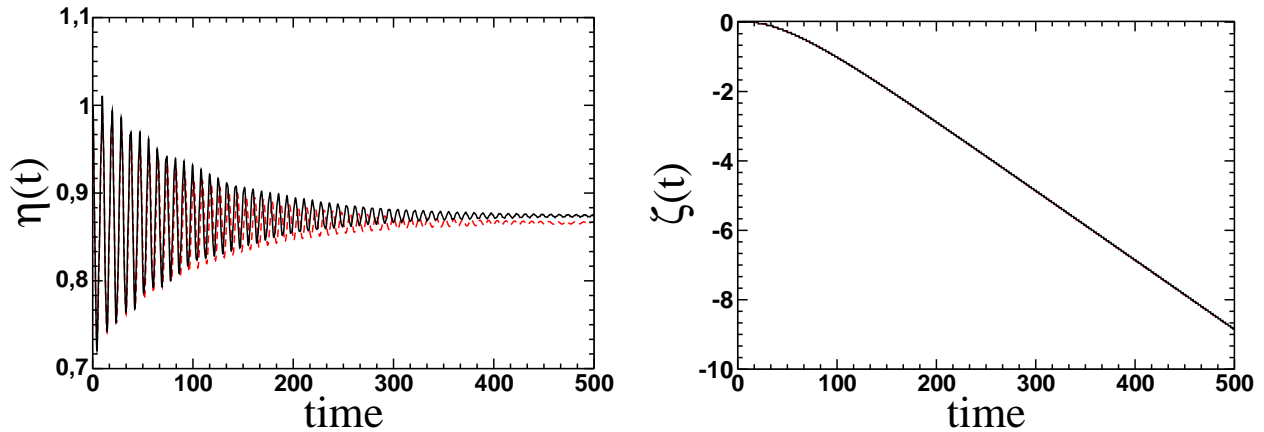


FIG. 2: (Color online). The amplitude and position of the soliton obtained from a simulation of the NLSE (red dashed lines) and from the numerical solution of the CC equations (solid lines). Parameters: $K = -0.01$, $a = 0.05$, $\delta = -3$, $\beta = 0.01$, with IC $\xi_0 = 0$, $\zeta_0 = 0$, $\phi_0 = \pi/2$ and $\eta_0 = 1$.

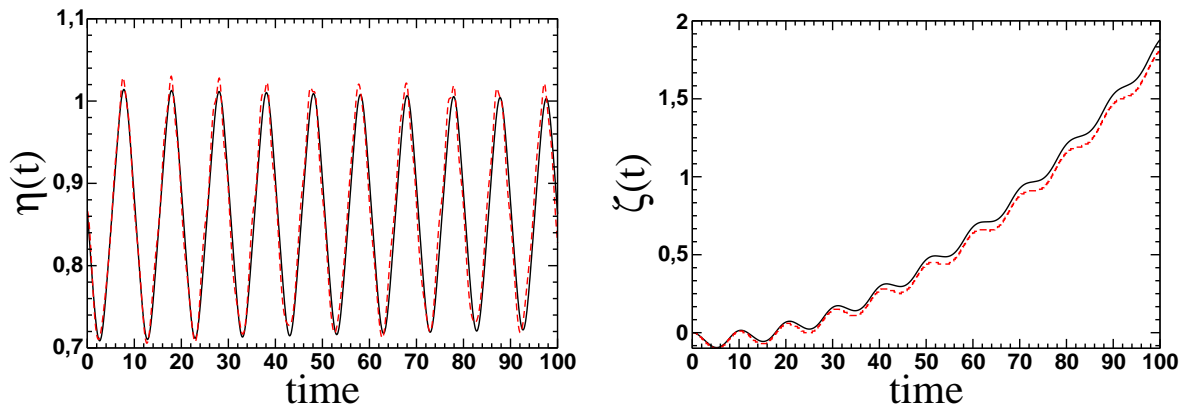


FIG. 3: (Color online). The amplitude and position of the soliton obtained from a simulation of the NLSE (red dashed lines) and from the numerical solution of the CC equations (solid lines). Parameters: $K = 0.1$, $a = 0.05$, $\delta = -3$, $\beta = 0.001$, with IC $\xi_0 = 0$, $\zeta_0 = 0$, $\phi_0 = 0$ and $\eta_0 = \sqrt{K^2 - \delta}/2$.

represent a strong perturbation for which the CC-theory can no longer be valid. Indeed, in the simulations the soliton soon becomes unstable.

V. OSCILLATORY SOLUTIONS

In order to study in more detail the intrinsic oscillations in the CCs (see previous section), we consider the case without damping ($\beta = 0$). Here oscillatory solutions are possible because the total energy (37) is conserved, see Eq. (42). This means that in Eq. (37) oscillations of the soliton energy, Eq. (23), are compensated by the oscillations of the term $2\pi a \operatorname{sech}A(t) \cdot \sin B(t)$ stemming from the perturbations. This is confirmed by inserting numerical solutions of the CC-equations.

In order to obtain analytical solutions our plan is to look first for stationary solutions and then to consider small oscillations around them. For the stationary solutions we make the ansatz $\zeta = \zeta_s + V_s t$, $\eta = \eta_s$, $\xi = \xi_s$ and $\phi = \phi_s - \alpha_s t$. The CC-equations (25), (28), (29), (30) yield

$$0 = -\frac{a\pi}{2} \operatorname{sech} A_s \cdot \cos B, \quad (44)$$

$$0 = aA_s \operatorname{sech} A_s \cdot \cos B, \quad (45)$$

$$V_s = -4\xi_s + \frac{a\pi^2}{8\eta_s^2} \operatorname{sech} A_s \cdot \tanh A_s \cdot \sin B, \quad (46)$$

$$-\alpha_s = 4(\xi_s^2 - \eta_s^2) - \delta + \frac{a\pi A_s}{2\eta_s} \operatorname{sech} A_s \cdot \tanh A_s \cdot \sin B, \quad (47)$$

with

$$A_s = \frac{\pi}{4}(K + 2\xi_s)/\eta_s, \quad (48)$$

$$B(t) = \phi_s + (K + 2\xi_s)\zeta_s + [(K + 2\xi_s)V_s - \alpha_s]t. \quad (49)$$

Eq. (44) must be fulfilled for arbitrary t , thus $\cos B \equiv 0$, which leads to

$$\alpha_s = (K + 2\xi_s)V_s, \quad (50)$$

$$\phi_s + (K + 2\xi_s)\zeta_s = \pm \frac{\pi}{2}, \quad (51)$$

$$\sin B = \pm 1, \quad (52)$$

respectively. In the following we can restrict ourselves to the case $\zeta_s = \xi_s = 0$, because other values yield qualitatively similar results (except of $\xi_s = -K/2$ which yields $\alpha_s = 0$ and thus the steady-state solution of Section IV). Using Eqs. (46), (47), (48) and (50) one transcendental equation for η_s remains:

$$4\eta_s^2 = -\delta \pm \frac{\pi^2 a K}{4\eta_s^2} \operatorname{sech} A_s \cdot \tanh A_s. \quad (53)$$

For the parameter set $a = 0.05$, $K = 0.1$ and $\delta = -3$ we get $\eta_s = 0.866239$ for $\phi_s = \pi/2$ and 0.865811 for $\phi_s = -\pi/2$. The numerical solution of the CC-equations for these two cases reveals that in the former case we have a stable stationary solution, whereas in the latter case the solution is unstable.

For the region around the stable stationary solution we expect that all CCs exhibit oscillations and we assume that these oscillations are harmonic if the amplitudes are sufficiently small. We choose $\phi_0 = \pi/2$ and make the ansatz

$$\zeta(t) = \bar{V}t - a_\zeta \sin(\Omega t), \quad (54)$$

$$\eta(t) = \eta_0 + a_\eta [1 - \cos(\Omega t)], \quad (55)$$

$$\xi(t) = -a_\xi [1 - \cos(\Omega t)], \quad (56)$$

$$\phi(t) = \phi_0 - \alpha t + a_\phi \sin(\Omega t). \quad (57)$$

This ansatz takes into account that the soliton first starts its oscillatory motion (i.e., $\zeta - \bar{V}t$ is linear in t for small t), then the soliton shape changes (i.e., η is quadratic for small t).

Since we have considered the stationary solution that belongs to $\xi_s = \zeta_s = 0$, we can neglect ξ compared to K and obtain for B in Eq. (27):

$$B = \phi_0 + (a_\phi - Ka_\zeta) \sin(\Omega t) + (K\bar{v} - \alpha)t. \quad (58)$$

Ka_ζ is one order smaller than a_ϕ , because $|K| \ll 1$, and we get

$$B = \phi_0 + a_\phi \sin(\Omega t) + (K\bar{V} - \alpha)t. \quad (59)$$

Here we can distinguish two limiting cases: In case 1 the linear terms cancel and we have a pure oscillatory behavior. In case 2 the linear term dominates the oscillatory term which can then be neglected. Indeed, taking the second derivative of ϕ with respect to time and using (25), (28), (29) and (30) one obtains $\ddot{\phi} = c_1 \sin(B) + c_2 \sin(2B) + c_3 \cos(B) + c_4 \cos(2B) + c_5$, where c_i with $i = 1, 2, \dots, 5$ are functions of the CCs. Considering the above approximations, and in addition when the terms of order of $aK\bar{V}(4\eta_0^2 + \delta)t$ are negligible, one realizes that c_1, c_2, c_4 and c_5 are small compared with $c_3 = \Omega^2$,

$$\Omega^2 \approx 4\pi a\eta_0, \quad (60)$$

and hence, the Eq. for $\phi(t)$ reads

$$\ddot{\phi} - \Omega^2 \cos(\phi) = 0. \quad (61)$$

Integrating this equation once we obtain

$$\dot{\phi} = \pm \Omega \sqrt{2} \sqrt{\sin(\phi) + C}, \quad (62)$$

where $C = \dot{\phi}_0^2/(2\Omega^2) - \sin(\phi_0) \approx ((4\eta_0^2 + \delta)^2)/(8\pi a\eta_0) - 1$. Then, if $C \gg 1$, the constant term dominates and so $\phi(t)$ goes linearly, i.e. $\phi(t) = \pi/2 \pm (4\eta_0^2 + \delta)t$. Notice that $C \gg 1$ implies $(4\eta_0^2 + \delta)^2 \gg 16\pi a\eta_0$, which can be solved for η_0 , yielding for $a = 0.05$, $\delta = -3$ and $\phi_0 = \pi/2$, $\eta_0 \ll 0.655$ or $\eta_0 \gg 1.077$. This is confirmed by numerical solutions of the CC-equations which exhibit an oscillatory behavior of $\phi(t)$ for $\eta_0 \in [0.65; 1.07]$, and a linear behavior (plus small oscillations) outside of this interval.

Finally we remark that both V_s in the stationary solution and \bar{V} in the oscillatory solutions differ from $V_f = 2K$ in Section IV. A transformation to a frame moving with $V \neq V_f$ would not simplify the NLSE because terms with Ψ_X would appear in Eq. (38).

VI. STABILITY OF OSCILLATORY SOLUTIONS

Our simulations reveal that the driven undamped soliton is stable only for a part of the solutions obtained by the CC-theory. Naturally we would like to predict, by using the CC-theory, which solutions are unstable and to understand what causes the instability (the latter point will be discussed in the next section).

For the NLSE-equation with a general local nonlinearity, but without driving and damping, the Vakhitov-Kolokolov stability criterion [15, 16] states that solitons are stable if $dN/d\Lambda > 0$. Here N is the norm and Λ the so-called spectral parameter in stationary solutions of the form $u(x, t) = \Psi(x) \exp(i\Lambda t)$. However, our oscillatory solutions, Eqs. (54)-(57) inserted into Eq. (17), have a more complicated time dependence; therefore the criterion cannot be applied here.

Instead, we apply the criterion of Pego and Weinstein [14] and show, by comparison with our simulations, that it works perfectly although this criterion was not derived for NLS-equations but for a large class of other soliton bearing equations: (generalized) Korteweg-de Vries equation, (generalized) Benjamin-Bona-Mahoney equation and (generalized, regularized) Boussinesq equation. The criterion was also successfully applied to a generalized Boussinesq equation with a non-local term stemming from long-range interactions in an anharmonic chain [18].

Pego and Weinstein proved for the above equations that the soliton becomes unstable, if

$$\frac{dP}{dV} < 0, \quad (63)$$

where P is the momentum of the soliton and V is its velocity. In the next section we will show that in our CC-theory the canonical momentum is identical to the kinetic momentum $P = -8\eta\xi$ in Eq. (24). The velocity $V = \dot{\zeta}$ is obtained by the r.h.s. of Eq. (29). In order to apply the criterion we only have to insert a (numerical) solution of the CC-equations and obtain $P(t)$ and $V(t)$, which is a parametric representation of the curve $P(V)$. As $\zeta(t)$ and $\phi(t)$, which contain contributions linear in t , do not appear in $P(t)$, and in $V(t)$ they appear only via $\sin B$, the functions $P(t)$ and $V(t)$ are periodic and therefore the curve $P(V)$ has a finite length. Plotting this “stability curve” we can immediately see whether the curve, or a branch of it, has a negative slope.

For the parameter set $a = 0.05$, $K = 0.1$, $\beta = 0$ and $\delta = -1$ and IC $\zeta_0 = \xi_0 = 0$ and $\phi_0 = \pi/2$, we find a small interval $0.48 \leq \eta_0 \leq 0.52$ with stable solutions around the stationary solution for $\eta_s = 0.501874$, as expected. There is another stable regime for $\eta_0 \geq 0.76$. When we go far away from the IC for the stationary solution by choosing $\phi_0 = 0$, instead of $\phi_0 = \pi/2$, the stability interval around η_s vanishes, as expected. The upper stability regime exists now for $\eta_0 \geq 0.69$.

When $|\delta|$ is increased, e.g. by choosing $\delta = -3$, the stability region around $\eta_s = 0.866239$ is much larger than in the case $\delta = -1$; for $\phi_0 = \pi/2$ it is $0.7 \leq \eta_0 \leq 1.03$. The upper stability region is above $\eta_0 = 1.08$. Considering again $\phi_0 = 0$, the stability region around η_s only shrinks to $0.76 \leq \eta_0 \leq 0.97$, but does not vanish because it was much larger than in the case $\delta = -1$. The upper stable region is above 1.02. Thus the conclusion is that *an increase of $|\delta|$ widens the regions with stable soliton solutions*. All stability regions given above are confirmed by simulations for the perturbed NLSE, with an error of less than 1 %.

At some of the boundaries of the above intervals there is a drastic change of the shape of the solutions of the CC-equations and the stability curve. E.g., for the first case above we obtain very anharmonic oscillations in all CCs for $\eta_0 = 0.75$ and the stability curve has a long branch with negative slope (Fig. 5). The simulations indeed show that the soliton becomes unstable very quickly and vanishes (Fig. 4). However, a slight change of η_0 to the value 0.76 produces a stability curve that has only one branch with a positive slope (Fig. 5). Here the soliton is indeed stable in the simulations (Fig. 6).

At the boundaries of other intervals the change of the shape of the solutions is less dramatic. E.g., for the case $\delta = -1$ and $\eta_0 = 0.46$ the oscillations in the CCs are small and harmonic. The stability curve has only a very short branch with negative slope which is visited in the time evolution only for very short time intervals (Fig. 7). Here the soliton is indeed stable for a relatively long time (Fig. 8). This soliton lifetime is increasingly reduced when η_0 is reduced by which the negative slope branch in $P(V)$ becomes longer. *Thus this curve predicts not only whether the soliton is stable, but also gives an estimate for its lifetime when it is unstable.*

VII. SOLITON AND PHONON DISPERSION CURVES

For the soliton dispersion curve $E^{sol}(P)$ we need the canonical momentum P of the soliton. P must fulfill the Hamilton equation

$$\dot{\zeta} = \frac{\partial H}{\partial P}, \quad (64)$$

where ζ is the soliton position. We start from the CC-Lagrangian Eq. (34) and obtain

$$\frac{\partial L}{\partial \dot{\phi}} = 4\eta = N, \quad (65)$$

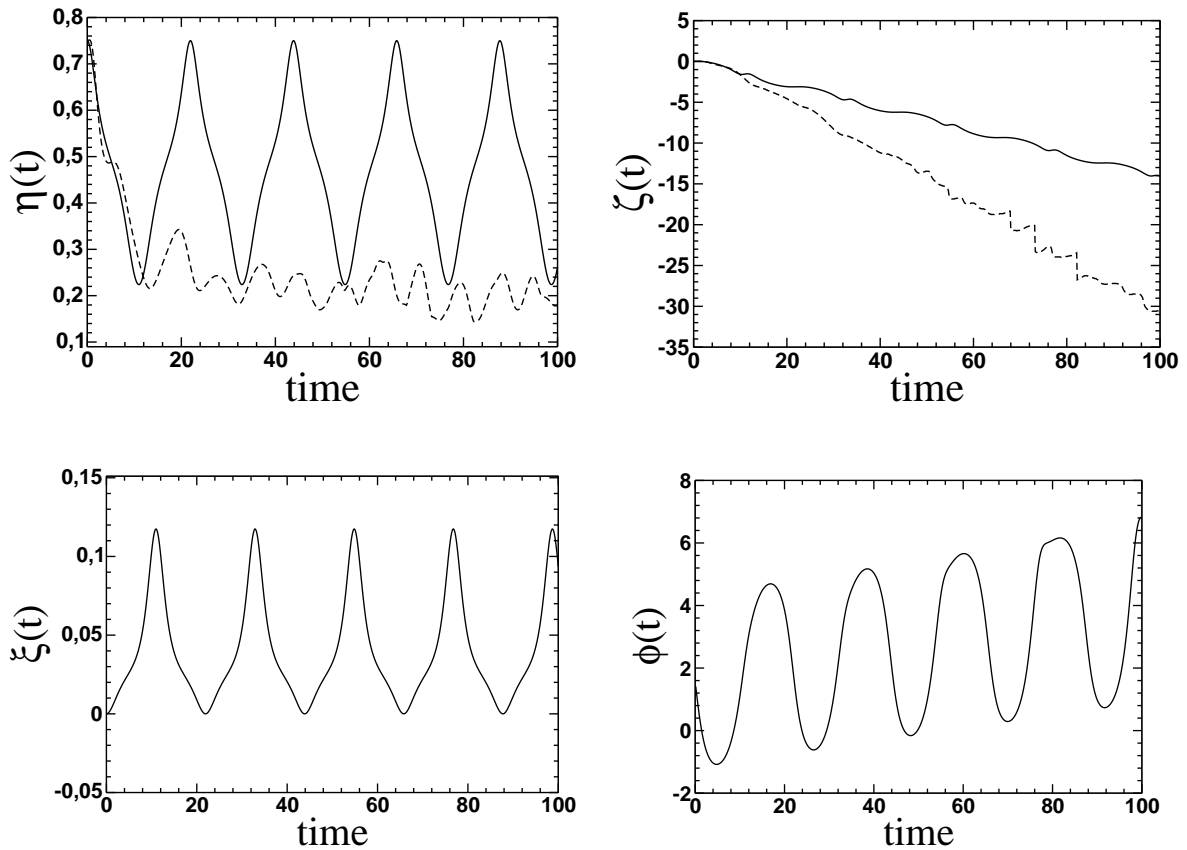


FIG. 4: The evolution of η , ζ , ξ and ϕ obtained from a simulation of the NLSE (dashed lines) and from the numerical solutions of the CC equations (solid lines). Parameters: $K = 0.1$, $a = 0.05$, $\delta = -1$, $\beta = 0$, with IC $\xi_0 = 0$, $\zeta_0 = 0$, $\phi_0 = \pi/2$ and $\eta_0 = 0.75$.

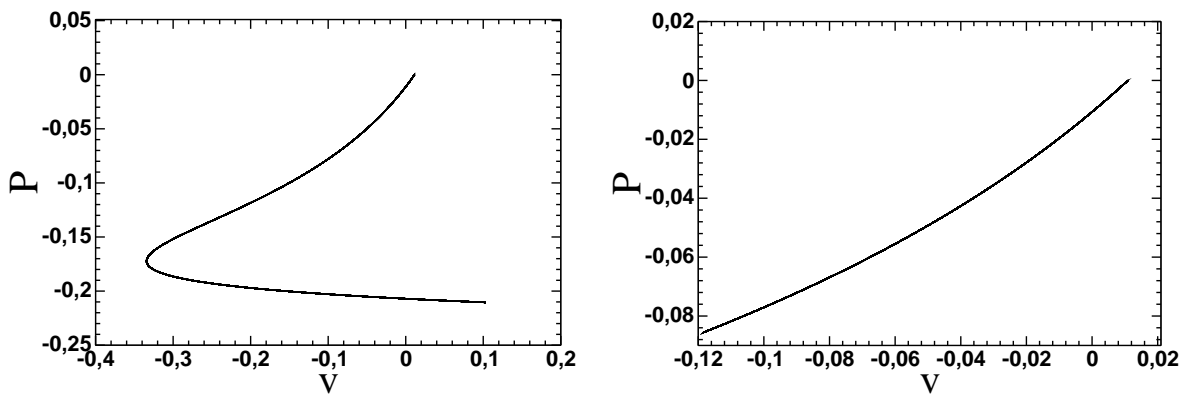


FIG. 5: “Stability curve” P versus V . Left panel: $\eta_0 = 0.75$. Right panel $\eta_0 = 0.76$. Other parameters as in Fig. 4.

as the angular momentum of the internal oscillation of the soliton, and

$$\frac{\partial L}{\partial \dot{\xi}} = 8\eta\zeta = 2N\zeta := X, \quad (66)$$

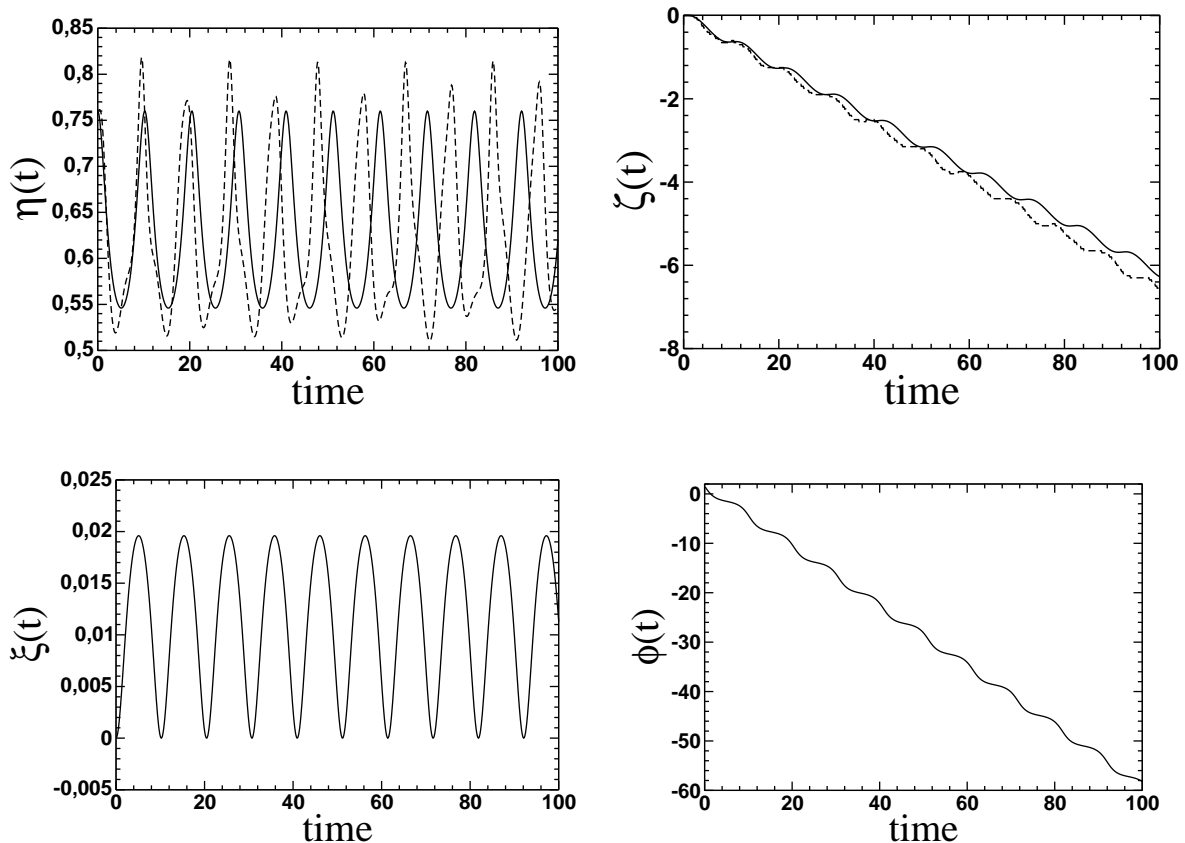


FIG. 6: The evolution of η , ζ , ξ and ϕ obtained from a simulation of the NLSE (dashed lines) and from the numerical solutions of the CC equations (solid lines). Parameters: $K = 0.1$, $a = 0.05$, $\delta = -1$, $\beta = 0$, with IC $\xi_0 = 0$, $\zeta_0 = 0$, $\phi_0 = \pi/2$ and $\eta_0 = 0.76$. The simulations were carried forward to a final time $t_f = 1000$.

as the variable which is canonically conjugate to ξ . Using a Legendre transformation we obtain the Hamilton function

$$H = X\dot{\xi} + N\dot{\phi} - L, \quad (67)$$

$$H(X, \xi; N, \phi) = 4N\xi^2 - \frac{1}{12}N^3 - \delta N + 2\pi a \operatorname{sech} A \cdot \sin B, \quad (68)$$

with

$$A = 2\pi \frac{K + 2\xi}{2N}, \quad B = \phi + \frac{K + 2\xi}{2N} X. \quad (69)$$

We now make an ansatz for a canonical transformation to the following new set of variables:

$$P = -2N\xi, \quad \zeta = \frac{1}{2N} X \quad (70)$$

$$\tilde{N} = N, \quad \tilde{\phi} = \phi + g(N, \xi, X). \quad (71)$$

This means that P is identical to the kinetic momentum in Eq. (24), \tilde{N} is chosen to be equal to N and g still has to be determined such that the four fundamental Poisson brackets are fulfilled. This yields $g = \xi X/N$. The new Hamiltonian reads

$$H(P, \zeta; N, \tilde{\phi}) = \frac{1}{N} P^2 - \frac{1}{12} N^3 - \delta N + 2\pi a \operatorname{sech} A \cdot \sin B, \quad (72)$$

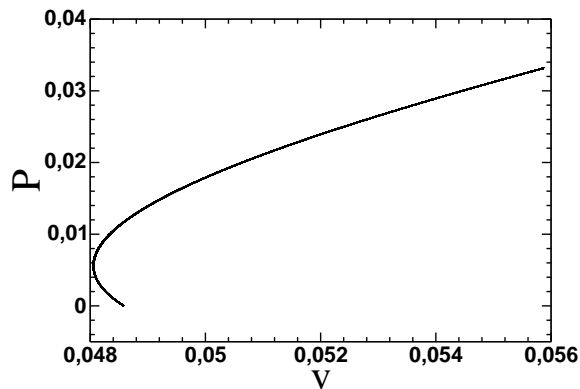


FIG. 7: “Stability curve” close to the boundary of an unstable regime. Parameters: $K = 0.1$, $a = 0.05$, $\delta = -1$, $\beta = 0$, with IC $\xi_0 = 0$, $\zeta_0 = 0$, $\phi_0 = \pi/2$ and $\eta_0 = 0.46$.

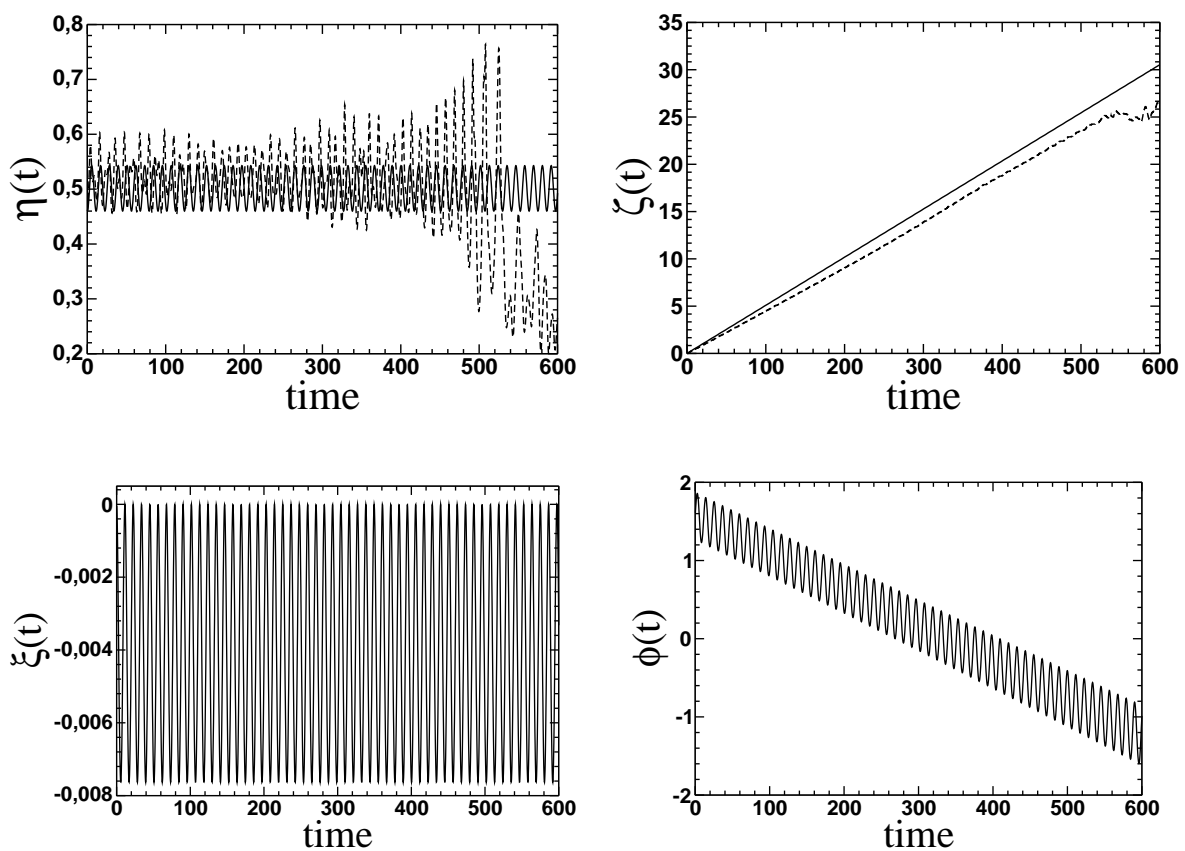


FIG. 8: The evolution of η , ζ , ξ and ϕ obtained from a simulation of the NLSE (dashed lines) and from the numerical solutions of the CC equations (solid lines). Parameters as in Fig. 7.

with

$$A = \frac{\pi}{N} \left(K - \frac{P}{N} \right), \quad B = \tilde{\phi} + K\zeta. \quad (73)$$

The first two terms in Eq. (72) agree with literature results on the unperturbed NLSE [3]. We have checked that the four Hamiltonian Eqs. which result from Eq. (72) are indeed equivalent to the four CC-equations in section III for the case without damping. The above results hold for the force $f(x, t)$ in Eq. (3) with arbitrary $K(t)$. In the following we return to the case of constant K in order to calculate analytically the stability and dispersion curves wherever it is possible.

Let us consider the stability intervals around the stationary solutions as given in Section VI. Except for the close vicinity to the boundaries, the oscillations in the CCs are nearly harmonic and can be well approximated by the Eqs. (54) to (57). Inserting into $P = -8\eta\xi$, neglecting the 2nd harmonic, and using $V = \dot{\zeta}$, one can easily see that $P(V)$ is a straight line with slope

$$\frac{dP}{dV} = \frac{8\eta_0 a_\xi}{\Omega a_\zeta} > 0, \quad (74)$$

because for $\eta_0 < \eta_s$ both a_ξ and a_ζ are positive and for $\eta_0 > \eta_s$ both are negative. The latter also holds for the upper stability regimes $\eta_0 \geq 0.76$ for $\delta = -1$ and $\eta_0 \geq 1.08$ for $\delta = -3$. In Section VI the case $\phi_0 = 0$ was also considered and two stability intervals $0.76 \leq \eta_0 \leq 0.97$ and $\eta_0 \geq 1.02$ appeared. Except for the boundary regions, $P(V)$ here also turns out to be linear, but the ansatz (54)-(57) has to be modified: First the shape of the soliton is changed, then it starts to move; whereas for $\phi_0 = \pi/2$ the soliton first starts to move, then the shape changes.

We now turn to the soliton dispersion curve $E^{sol}(P)$. Both $P = -8\eta\xi$ and E^{sol} in Eq. (23) consist of powers of η and ξ . For the following it is sufficient to approximate $\eta \approx \bar{\eta} + a_\eta \sin(\Omega t)$ and $\xi \approx \bar{\xi} + a_\xi \sin(\Omega t)$ where $\bar{\xi}$ is negligible; here a phase in $\sin(\Omega t)$ has been omitted because it is not relevant for the following. We concentrate on the leading terms in $\sin(\Omega t)$ and distinguish two cases: In case I both $E^{sol}(t)$ and $P(t)$ have a leading term with $\sin(\Omega t)$; in this case the dispersion curve $E^{sol}(P)$ is linear in the first approximation. In case II the 1st-order terms in $E^{sol}(t)$ cancel if $\bar{\eta} = \frac{1}{2}\sqrt{-\delta}$, but cannot cancel in $P(t)$. In the next order

$$E^{sol}(t) = E_{max} - \Delta E \sin^2(\Omega t), \quad (75)$$

with $\Delta E = 16\bar{\eta}(a_\eta^2/3 - a_\xi^2) > 0$ because $|a_\xi| \ll |a_\eta|$. Inserting $P = \bar{P} + 8\bar{\eta}a_\xi \sin(\Omega t)$ yields a parabolic dispersion curve

$$E^{sol}(t) = E_{max} - \Delta E \left(\frac{P - \bar{P}}{8\bar{\eta}a_\xi} \right)^2. \quad (76)$$

This turns out to be a surprisingly good approximation when comparing with the dispersion curve obtained by using numerical solutions for $\eta(t)$ and $\xi(t)$, even when the cancellation of the linear terms in $E^{sol}(t)$ is not exact. The condition $\bar{\eta} = \sqrt{-\delta}/2$ is approximately fulfilled for the regions with strong oscillatory terms in $\phi(t)$; see end of Section V.

When solitons become unstable they radiate phonons (i.e., linear excitations). Therefore we consider the perturbed linearized NLSE without damping

$$iu_t + u_{xx} + \delta u = a e^{iKx}, \quad (77)$$

which is solved by

$$u(x, t) = c e^{i(kx - \omega_k t)} + b e^{i(Kx - \omega_K t)} - \frac{a}{\omega_K} e^{iKx} \quad (78)$$

with $\omega_k = k^2 - \delta$, $\omega_K = K^2 - \delta$. The first term in Eq. (78) represents the phonons of the unperturbed equation with the free amplitude c and the dispersion curve ω_k .

The second term in Eq. (78) with the free amplitude b represents a single phonon mode whose wave number and frequency are given by the parameter K in the force $f(x) = a e^{iKx}$. Such phonons are typically radiated at the beginning of a simulation when the initial soliton profile adapts to the system. These phonons can be observed best when they interact with the soliton after having been reflected by a boundary of the system.

Finally, the last term in Eq. (78) represents a static background with a fixed amplitude a/ω_K . This was already discussed below Eq. (43).

VIII. CONCLUSIONS

We have considered the dynamics of NLS-solitons in one spatial dimension under the influence of non-parametric spatio-temporal forces of the form $f(x, t) = a \exp[iK(t)x]$, plus a damping term and a linear term $\delta u(x, t)$ which stabilizes the driven soliton. We have developed a CC-theory which yields a set of ODEs for the four CCs (position ζ , velocity ξ , amplitude η , and phase ϕ).

These ODEs have been solved analytically and numerically for the case of a constant, spatially periodic force $f(x) = a \exp[iKx]$. The soliton position exhibits oscillations around a mean trajectory $\bar{\zeta} = \bar{V}t$; this means that the soliton performs, on the average, a unidirectional motion although the spatial average of the force vanishes. The amplitude of the oscillations is much smaller than the spatial period $L = 2\pi/|K|$ of the inhomogeneity $f(x)$. The other three CCs also exhibit oscillations with the same frequency as in $\zeta(t)$.

In the case of damping, the above oscillations are damped and the solution approaches a steady-state solution with constant velocity, if the IC are close enough to those of the steady-state solution and if the damping is not too large. Otherwise the soliton vanishes, i.e. its amplitude and energy go to zero while its width goes to infinity.

In the case without damping all the above oscillations persist. These periodic solutions exist because the total energy of the *perturbed* system is a conserved quantity, even for *arbitrary* inhomogeneity $f(x)$, and independent of the CC-ansatz.

However, a comparison with simulation results for the perturbed NLSE reveals that only part of the above oscillatory solutions are stable. Our CC-theory predicts the unstable regions in the IC and the parameters with high accuracy, by using the instability criterion of Pego and Weinstein. This criterion predicts instability if the slope of the curve $P(V)$ becomes negative somewhere, here P and V are the soliton momentum and velocity, respectively. It turns out that the stability regions become broader when the parameter δ is chosen more negative. Moreover, we have found out that the curve $P(V)$ also yields a good estimate for the soliton lifetime: The soliton lives the longer, the shorter the negative-slope branch is, as compared to the length of the positive-slope branch.

Other cases of the force $f(x, t) = \exp[iK(t)x]$ will be considered in a second paper: specifically single and biharmonic $K(t)$, with and without damping.

IX. ACKNOWLEDGMENTS

We thank Yuri Gaididei (Kiev) and Angel Sánchez (Madrid) for useful discussions on this work. F.G.M. acknowledges the hospitality of the University of Sevilla and of the Theoretical Division and Center for Nonlinear Studies at Los Alamos Laboratory. Work at Los Alamos is supported by the USDOE. We acknowledge financial support by the Ministerio de Educación y Ciencia (MEC, Spain) through FIS2008-02380/FIS, and by the Junta de Andalucía under the projects FQM207(NRQ),

FQM-00481 and P06-FQM-01735 (NRQ).

- [1] Y. Kivshar and B. Malomed, *Rev. Mod. Phys.* **61**, 763 (1989).
- [2] B. Malomed, *Prog. in Optics* **43**, 69 (2002).
- [3] L. D. Faddeev, L. Takhtajan, *Hamiltonian methods in the theory of solitons*, Classics in Mathematics, Springer-Verlag, Berlin (2007).
- [4] I. V. Barashenkov, M. M. Bogdan, and V. I. Korobov, *Europhys. Lett.* **15**, 113 (1991).
- [5] M. Bondila, I. V. Barashenkov, and M. M. Bogdan, *Physica D* **87**, 314 (1995).
- [6] R. Scharf and A. R. Bishop, *Phys. Rev. E* **47**, 1375 (1993).
- [7] D. Poletti, E. A. Ostrovskaya, T. J. Alexander, B. Li, Y. S. Kivshar, *Physica D* **238**, 1338 (2009).
- [8] D. J. Kaup and A. C. Newell, *Proc. R. Soc. London A* **361**, 413 (1978), *Phys. Rev. B* **18**, 5162 (1978).
- [9] I. V. Barashenkov, and Yu. S. Smirnov, *Phys. Rev. E* **54**, 5707 (1996).
- [10] I. V. Barashenkov, and E. V. Zemlyanaya, *Physica D* **132**, 363 (1999).
- [11] G. Cohen, *Phys. Rev. E* **61**, 874 (2000).
- [12] V. M. Vyas, T. S. Raju, C. N. Kumar, and P. K. Panigrahi, *J. Phys. A* **39**, 9151 (2006).
- [13] A. Gorbach, S. Denisov, and S. Flach, *Opt. Lett.* **31**, 1702 (2006).
- [14] R. L. Pego and M. I. Weinstein, *Phil. Trans. R. Soc. London A* **340**, 47 (1992).
- [15] N. G. Vakhitov and A. A. Kolokolov, *Radiophys. Quantum Electron.* **16**, 783 (1975).
- [16] M. I. Weinstein, *Comm. Pure Appl. Math.* **39**, 51 (1986).
- [17] MATHEMATICA 5.2 (Wolfram Research Inc., Champaign).
- [18] Y. Gaididei, N. Flytzanis, A. Neuper and F. G. Mertens, *Physica D* **107**, 83 (1997).